Organic & Biomolecular Chemistry

PAPER

View Article Online
View Journal

Cite this: DOI: 10.1039/c6ob01375a

Biomimetic deiodination of thyroid hormones and iodothyronamines – a structure–activity relationship study†

Santanu Mondal and Govindasamy Mugesh*

Received 25th June 2016,
Accepted 9th August 2016

DOI: 10.1039/c6ob01375a

www.rsc.org/obc

Mammalian selenoenzymes, iodothyronine deiodinases (DIOs), catalyze the tyrosyl and phenolic ring deiodination of thyroid hormones (THs) and play an important role in maintaining the TH concentration throughout the body. These enzymes also accept the decarboxylated thyroid hormone metabolites, iodothyronamines (TAMs), as substrates for deiodination. Naphthalene-based selenium and/or sulphur-containing small molecules have been shown to mediate the regioselective tyrosyl ring deiodination of thyroid hormones and their metabolites. Herein, we report on the structure–activity relationship studies of a series of *peri*-substituted selenium-containing naphthalene derivatives for the deiodination of thyroid hormones and iodothyronamines. Single crystal X-ray crystallographic and ^{77}Se NMR spectroscopic studies indicated that the intramolecular Se···X (X = N, O and S) interactions play an important role in the deiodinase activity of the synthetic mimics. Furthermore, the decarboxylated metabolites, TAMs, have been observed to undergo slower tyrosyl ring deiodination than THs by naphthyl-based selenium and/or sulphur-containing synthetic deiodinase mimics and this has been explained on the basis of the strength of Se···I halogen bonding formed by THs and TAMs.

Introduction

Regioselective monodeiodination of L-thyroxine or 3,3′,5,5′-tetraiodothyronine (T4), the major prohormone secreted by the thyroid gland, plays an important role in thyroid hormone homeostasis. T4 can undergo monodeiodination at its phenolic and tyrosyl ring to produce the biologically active and inactive metabolites 3,3′,5-triiodothyronine (T3) and 3,3′,5′-triiodothyronine (rT3), respectively.[1] Similarly, removal of one iodine from the tyrosyl- and phenolic rings of T3 and rT3, respectively, is also known to produce a biologically inactive metabolite 3,3′-diiodothyronine (3,3′-T2) (Scheme 1). These regioselective deiodinations of thyroid hormones (THs) are catalysed by three isoforms of a selenoenzyme, iodothyronine deiodinase type 1 (DIO1), type 2 (DIO2) and type 3 (DIO3). While DIO1 can remove iodine from both the tyrosyl and phenolic rings, DIO2 and DIO3 are selective towards phenolic

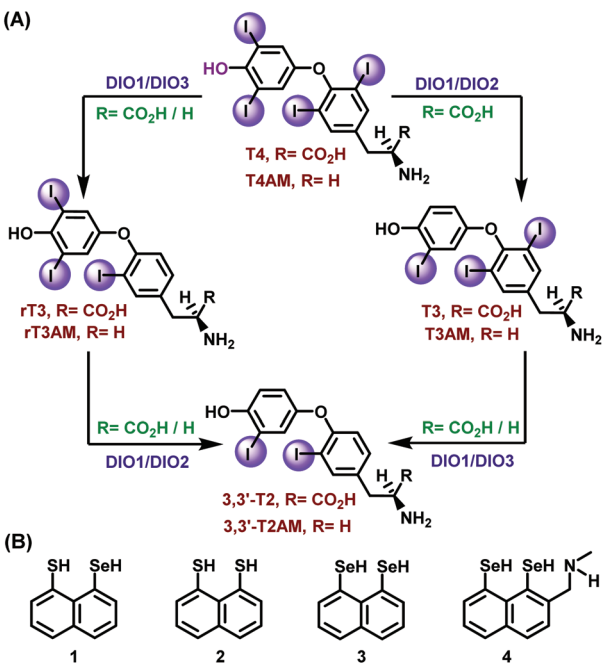

Scheme 1 (A) Biochemical deiodination of thyroid hormones and iodothyronines by iodothyronine deiodinases (DIOs). (B) Chemical structures of compounds **1–4**.

Department of Inorganic and Physical Chemistry, Indian Institute of Science, Bangalore 560012, India. E-mail: mugesh@ipc.iisc.ernet.in

†Electronic supplementary information (ESI) available: NMR characterisation data, mass spectra, HPLC chromatograms, coordinates of optimized geometries. CCDC 1486467 and 1486468. For ESI and crystallographic data in CIF or other electronic format see DOI: 10.1039/c6ob01375a

and tyrosyl ring deiodinations, respectively.[2–4] Although all the three isoforms have a very similar amino acid sequence in the active site, the origin of the regioselectivity of deiodination is still not clear. Although DIO-catalysed biochemical deiodinations have been discovered as the major metabolic pathways, THs also undergo decarboxylation to form iodothyronamines (TAMs).

Although there can be a total of nine iodothyronamines depending on the number and position of the iodine atoms, only 3-iodothyronamine (3-T1AM) and thyronamine (T0AM) could be detected so far in the blood plasma of various organisms.[5a] These two metabolites have been shown to induce hypothermia, hyperglycemia and bradycardia in mice when injected in pharmacological doses.[5a,b] They are also known to activate trace amine-associated receptor 1 (TAAR1), an orphan G-protein coupled receptor, and inhibit the neoronal reuptake of the neurotransmitter dopamine and the norepinephrine by dopamine transporter (DAT) and the norepinephrine transporter (NET), respectively.[6,7] Recently, TAMs have been shown to be isozyme-specific substrates of iodothyronine deiodinases (DIOs) (Scheme 1) although some of the TAMs do not undergo deiodination by DIOs.[8]

Recently, our efforts in the development of naphthyl-based selenium and/or sulphur-containing compounds (**1–4**) as functional mimics of DIO3 have attracted significant research attention.[9] Compounds **1–4** mediate regioselective tyrosyl ring deiodination of T4 and T3 to produce rT3 and 3,3′-T2, respectively. These compounds are also found to mediate the deiodination of thyroid hormone metabolites such as iodothyronine sulphates and iodothyronamines, and iodinated nucleosides.[9d–f] Deiodinase activity of these compounds has been explained by the cooperative action of Se···I halogen bonding and the chalocogen bonding interaction between two nearby chalocogen atoms. Noncovalent Se···N interaction between the amine group and the nearby selenium atom in compound **4** was shown to increase the deiodinase activity of the compound. Herein, we report the effect of different heteroatom-containing substituents on the deiodination activity of naphthalene derivatives for the deiodination of thyroid hormones and iodothyronamines. We also show that the carboxylic acid group in the β-alanine side chain of thyroid hormones has a significant effect on the biomimetic deiodination reactions.

Results and discussion

Deiodination of THs and TAMs in the presence of dithiothreitol was carried out by naphthyl-based diselenols **5–10** having a lone pair-containing atom such as nitrogen, oxygen and sulphur in the close proximity of one of the selenols (Scheme 2). Compounds **5–10** were freshly generated in the assay mixture by reducing the corresponding diselenides **12–17** (Scheme 2) with sodium borohydride ($NaBH_4$). All of these compounds were synthesized from the aldehyde **18** or **19** (Scheme S1, ESI†). **18** was refluxed with the primary amines to produce the Schiff bases **20** and **21**, which were further reduced with $NaBH_4$ to afford the amine-substituted compounds **12** and **13**, respectively. *ortho*-Substituted aldehyde **18** was reduced with $NaBH_4$ to produce compound **14**. Compounds **15–17** were synthesized by borontrifluoride–diethyl etherate (BF_3–Et_2O) catalysed thioacetal formation by **18** in the presence of thiols.

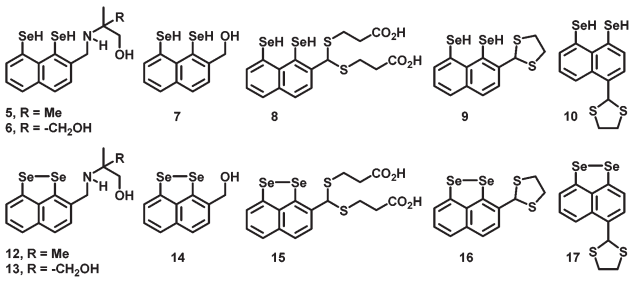

Scheme 2 Chemical structures of **5–10** and **12–17**.

The deiodination reactions were monitored by high pressure liquid chromatography (HPLC) and the deiodinated products were quantified by comparing the peak area with that of standard samples. Due to the low solubility of the TAMs in sodium phosphate buffer (100 mM) at physiological pH, deiodination reactions were performed in a mixture of sodium phosphate buffer (100 mM, pH 7.00) and 20% v/v acetonitrile.

Under these assay conditions, T4 readily underwent deiodination by all the compounds **5–10** to form rT3. The initial rate of deiodination was determined by monitoring the initial 10–15% conversion of the starting material to the product. The initial rates of deiodination of T4 by compound **5** and **6** are 2.6 and 1.9 times, respectively, higher than that of the parent compound **3** (Fig. 1 and Table S1, ESI†). These results are in agreement with our previous observation that the introduction of a secondary amine group in the close proximity of one of the selenols in **3** increases the deiodination activity. The deiodination of T4 by compound **7** (Fig. 1 and Table S1, ESI†)

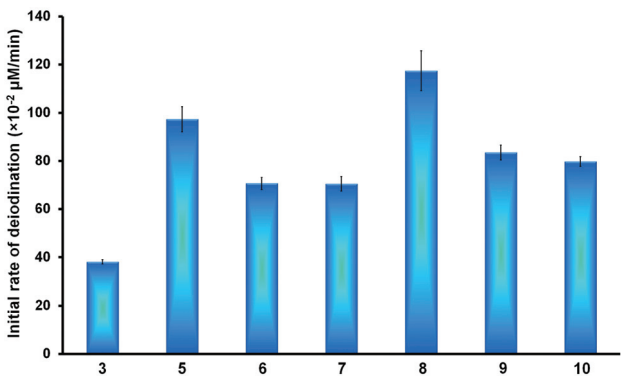

Fig. 1 Comparison of initial rates of deiodination of T4 by compounds **3** and **5–10**. Assay conditions: T4 (0.3 mM), mimics (1.2 mM), dithiothreitol (DTT) (15 mM), sodium borohydride ($NaBH_4$) (30 mM), sodium phosphate buffer (100 mM, pH 7.0), 20% acetonitrile (v/v), 37 °C.

is also faster than that by the parent compound **3**, indicating that the presence of an alcohol moiety can also facilitate the deiodination reactions. Interestingly, compound **8**, with thioacetal substitution, exhibits the highest deiodination activity in the series for the deiodination of T4. The initial rate of deiodination of T4 by compound **8** is almost 3 times higher than that of the parent compound **3**. However, the deiodination activities of the other thioacetal-based compounds **9** and **10** are 1.4 and 1.5 times, respectively, lower than that of compound **8** (Fig. 1 and Table S1, ESI†). In contrast to the deiodination of T4, T4AM does not undergo deiodination by compounds **3** and **5–10** (Fig. S29A, ESI†). As the addition of T4AM to phosphate buffer (100 mM, pH 7.0) makes the solution turbid, the deiodination of T4AM has been carried out in acetonitrile in which it is completely soluble. In fact, T4AM undergoes both the tyrosyl and phenolic ring deiodination to form rT3AM and T3AM, respectively, by all the compounds in acetonitrile, indicating that the solvent has a significant effect on the regioselectivity of deiodination reactions (Fig. S29B, ESI†).

Deiodination of THs by naphthyl-based diselenols was explained by the co-operative action of halogen bonding and chalcogen bonding.[9c] While the Se···I halogen bonding interaction elongates the C–I bond, chalcogen bonding between two selenium atoms increases the strength of the halogen bonding between selenium and iodine. Strong Se···N noncovalent interaction in the amino-substituted naphthyl-based diselenol **4** increases the deiodination activity by supplying electron density to the selenium atom close to nitrogen and therefore, further strengthening the halogen bonding as well as chalcogen bonding interactions.[9c] Compounds **5–10** were designed on the basis of Se···X (X = N, O and S) interactions that can enhance the activity of these compounds in deiodinating thyroid hormones and iodothyronamines. The presence of Se···X (X = N, O and S) interactions in compounds **5–10** and their oxidized precursors **12–17** can be understood from the ^{77}Se chemical shifts. The signal for one of the selenols in **6** (δ = 91 ppm) is shifted upfield significantly relative to the other selenol (δ = 212 ppm) in the same compound or **3** (δ = 156 ppm) (Table 1). This indicates the more nucleophilic character of the selenol adjacent to the secondary amine moiety as compared to the other selenol moiety. Similarly, the signal for the selenol adjacent to the oxygen atom in **7** and sulphur atoms in **11** appear at more upfield regions δ = 52 ppm and δ = 72 ppm, respectively (Table 1). These results indicate that the Se···O and Se···S interactions can increase the nucleophilicity of the proximal selenol more than the Se···N interaction does in **5** and **6**. In compound **9**, the selenol moiety adjacent to the thioacetal ring appears at δ = 102 ppm, indicating that the Se···S interaction is weak due to the rigidity of the five-membered ring (Table 1). Although compound **10** does not contain an intramolecular Se···S interaction, the ^{77}Se signals for this compound indicate the possible intermolecular Se···S interactions in solution.

However, it is not clear why compound **5** exhibits two upfield-shifted peaks (δ = 91 ppm and 86 ppm), whereas the corresponding oxidized compound **12** exhibits only one upfield-shifted peak at δ = 345 ppm in the ^{77}Se NMR.

The presence of Se···X (X = N, O and S) interactions was also observed in the X-ray structure of the oxidized precursors of deiodinase mimics. The single crystal X-ray structure of compound **13** exhibited a strong Se···N interaction with a Se···N nonbonded distance of 2.563 Å, which is almost 25.8% shorter than the sum of van der Waals radii of selenium and nitrogen (3.45 Å) (Fig. 2A).[10] Similarly, a strong Se···O noncovalent interaction was observed in the single crystal X-ray structure of compound **14** (Fig. 2B). The non-bonded distance between the selenium and oxygen atom in **14** has been observed to be 2.818 Å, which is almost 17.6% shorter than the sum of van der Waals radii of selenium and oxygen (3.42 Å). One of the sulphur atoms in the thioacetal-based compound **16** interacts strongly with the nearby selenium with a Se···S non-bonded distance of 3.090 Å.[9d] The other sulphur atom in the five-membered ring of compound **16** interacts very weakly with the nearby selenium atom.

The strength of the Se···X (X = N, O and S) interaction in compounds **5–10** correlates well with the observed deiodination activity. Compounds **5–7**, with the secondary amine and hydroxymethyl substitutions, exhibit higher deiodination activity compared to the parent compound **3**. Thioacetal-based

Table 1 Chemical shifts (δ) in the ^{77}Se NMR spectra of compounds **3** and **5–17**

Compound[a]	Chemical shift[b] (δ, ppm)	Compound[a]	Chemical shift[b] (δ, ppm)
3	156	**11**	415
5	86, 91, 217	**12**	345, 426
6	91, 212	**13**	342, 439
7	52, 211	**14**	406, 411
8	73, 198	**15**	390, 446
9	102, 205	**16**	382, 453
10	96, 199	**17**	381, 453

[a] Selenols **3** and **5–10** were generated by reducing the corresponding diselenides **11–17** with sodium borohydride ($NaBH_4$). The chemical structure of compound **11** has been shown in the ESI (Scheme S1). [b] ^{77}Se chemical shifts of the selenols and diselenides were recorded in a mixture of 1 : 1 chloroform and methanol.

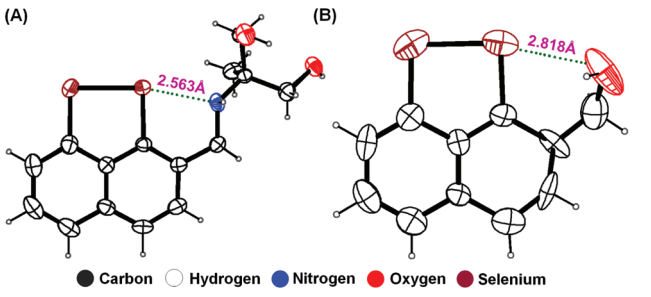

Fig. 2 ORTEP representation of the single crystal X-ray structures of compounds **13** (A) and **14** (B) showing the Se···N and Se···O interactions, respectively. The thermal ellipsoids are drawn at 50% probability.

compound **8** exhibits the highest deiodination activity in the series for the deiodination of T4 (Fig. 1 and Table S1, ESI†). As sulphur is more polarisable than nitrogen and oxygen, it may interact more strongly with the nearby selenium atom, which becomes electron-deficient due to halogen bonding and chalcogen bonding interactions. Furthermore, a closer orbital matching between the sulphur and selenium atom may also lead to more effective electron donation from sulphur than from nitrogen or oxygen to the nearby selenium atom. Compound **9**, with a rigid five-membered ring, exhibits weaker Se···S interaction and therefore, a lower deiodination activity than compound **8** is expected. Compound **10**, which lacks the intramolecular Se···S interaction but could potentially have intermolecular Se···S interactions, also exhibits lower deiodination activity than compounds **8** and **9** for the deiodination of T4 (Fig. 1 and Table S1, ESI†).

Deiodination of the triiodo-derivatives, T3 and T3AM, were also checked with compounds **3** and **5–10**. Interestingly, all these compounds mediate the tyrosyl ring deiodination of T3 and T3AM, to form 3,3′-T2 and 3,3′-T2AM, respectively. Similar to the deiodination of T4, the initial rates of deiodination of T3 by compounds **5** and **6** are higher than that by the parent compound **3** (Fig. 3 and Table S1, ESI†). In contrast to the deiodination of T4, the activity of compound **7**, exhibiting Se···O interaction, is found to be more than that of **5** and **6**, which exhibits Se···N interaction, for the deiodination of T3. Furthermore, the rate of deiodination of T3 by compound **7** is 1.5 times more than that by the parent compound **3** (Fig. 3 and Table S1, ESI†). Thioacetal-based compound **8** with a sulphur-containing flexible side chain exhibits the highest deiodination activity of the series. The rate of deiodination of T3 by compound **8** has been found to be 2.3 times more than that by the parent compound **3** indicating that the presence of polarizable sulphur atoms in the close proximity of selenium facilitates the deiodination reaction by *peri*-substituted naphthalene derivatives. Similar to the deiodination of T4, compounds **9** and **10** exhibit lower deiodination activity than compound **8** for the deiodination of T3.

Deiodination of T3AM by compounds **3** and **5–10** follow almost similar trends to that described for T3. Compounds **5–7**, with amino and hydroxymethyl substitutions, mediate faster deiodination of T3AM than the parent compound **3** (Fig. 3 and Table S1, ESI†). The thioacetal-based compound **8** exhibits the highest activity in the series for the deiodination of T3AM (Table 1). Interestingly, the deiodination of T3 by compounds **3** and **5–10** has been observed to be almost 4–11 times faster than that of T3AM, indicating that the removal of the carboxylate group from the β-alanine side chain of T3 decreases the rate of deiodination (Fig. 3 and Table S1, ESI†). These results are quite similar to our previous observations that T3AM undergoes slower deiodination by synthetic organoselenium compounds than T3.[9d] It should be noted that T3AM also undergoes slower tyrosyl ring deiodination by DIO3 than T3.[8] Interestingly, the other triiodo derivative, rT3AM does not undergo deiodination by the naphthyl-based deiodinase mimics (Fig. S30B, ESI†), which is very similar to our previous observation that rT3 does not undergo deiodination by deiodinase mimics.

The diiodo derivative, 3,5-diiodothyronine (3,5-T2), with both the iodine atoms in the tyrosyl ring (Fig. 4A), exhibits interesting pharmacological and thyromimetic[11] properties.

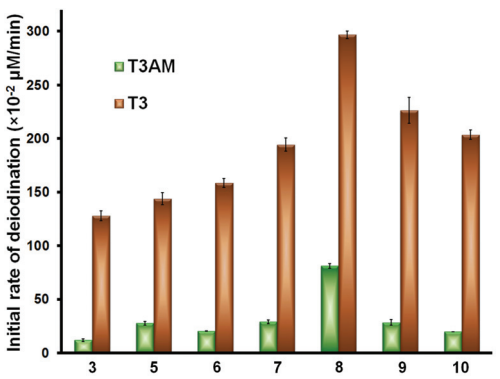

Fig. 3 Comparison of initial rates of deiodination of T3 and T3AM by compounds **3** and **5–10**. Assay conditions: T3 or T3AM (0.3 mM), mimics (1.2 mM), dithiothreitol (DTT) (15 mM), sodium borohydride ($NaBH_4$) (30 mM), sodium phosphate buffer (100 mM, pH 7.0), 20% acetonitrile (v/v), 37 °C.

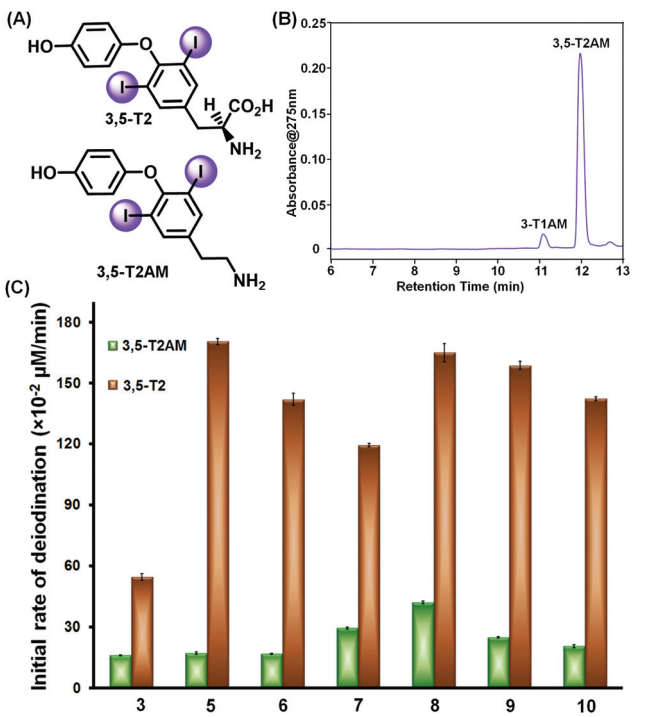

Fig. 4 (A) Chemical structures of 3,5-T2 and 3,5-T2AM. (B) HPLC chromatogram of the deiodination of 3,5-T2AM by compound **3**. (C) Comparison of initial rates of deiodination of 3,5-T2 and 3,5-T2AM by compounds **3** and **5–10**. Assay conditions: 3,5-T2 or 3,5-T2AM (0.3 mM), mimics (1.2 mM), dithiothreitol (DTT) (15 mM), sodium borohydride ($NaBH_4$) (30 mM), sodium phosphate buffer (100 mM, pH 7.0), 20% acetonitrile (v/v), 37 °C.

Chronic administration of 3,5-T2 in Wistar rats has been shown to significantly reduce the thyroidal iodide uptake, thyroperoxidase (TPO)-activity, NADPH oxidase 4 (NOX 4)-activity, DIO1-activity and to increase the expression of thyroid stimulating hormone (TSH) receptor and dual oxidase (DUOX)-activity.[12] Regular dosage of 3,5-T2 in rats also leads to decrease in TSH, T3 and T4 concentration. Intraperitoneal (i.p.) administration of 3,5-T2 in Wistar rats, receiving fat enriched diet, results in a significant reduction in the adiposity and body-weight gain without altering the serum TSH, T3 and T4 concentration.[13] 3,5-T2 also exhibits remarkable thyromimetic activity in the *in vitro* assays involving nuclear receptors (TRs) and GH3 cells.[14] However, the biosynthesis of 3,5-T2 is still not clear. Homogenates of NCLP-6E monkey hepatocarcinoma cells expressing DIO1 enzymatic activity has been reported to mediate phenolic ring deiodination of T3 to produce 3,5-T2, although T3 has been excluded as the substrate for phenolic ring deiodination by DIO1 in many experiments.[15]

Herein, we show, for the first time, that 3,5-T2 and its decarboxylated metabolite, 3,5-T2AM (Fig. 4A) can undergo regioselective tyrosyl ring deiodination by naphthyl-based deiodinase mimics to form 3-iodothyronine (3-T1) and 3-iodothyronamine (3-T1AM), respectively. These deiodination reactions were also monitored by HPLC (Fig. 4B) and the formation of deiodinated products was confirmed by comparing the HPLC chromatogram with that of a standard sample of the expected deiodinated product as well as mass spectral analysis. Comparison of the initial rates of deiodination of 3,5-T2 by compounds **3** and **5–10** indicates that compounds **5–7** exhibit higher deiodination activity than the parent compound **3** (Fig. 4C and Table S1, ESI†). Although compound **8** exhibits the highest activity in the series, the activity of compounds **9** and **10** has been found to be almost similar to or slightly lower than that of compound **8**, which is in contrast to the deiodination of T4, T3 and T3AM by compounds **8–10** (Table S1, ESI†). Interestingly, unlike the deiodination of 3,5-T2, compounds **5** and **6** exhibit almost similar deiodination activity as the parent compound **3** for the deiodination of 3,5-T2AM (Fig. 4C and Table S1, ESI†). Furthermore, in contrast to the deiodination of 3,5-T2, the deiodination activity of compound **9** is significantly lower than that of compound **8** for the deiodination of 3,5-T2AM. These results indicate that in addition to the Se···X (X = N, O and S) interactions, the deiodinase activity of compounds **5–10** also depends on the nature of the substrates. Similar to the differences in the rate of deiodination of T3 and T3AM, deiodination of 3,5-T2 by compounds **3** and **5–10** has been found to be 3–10 times faster than that of 3,5-T2AM (Fig. 4C and Table S1, ESI†). Furthermore, the deiodination of T3 and T3AM by the naphthyl-based deiodinase mimics is faster than that of 3,5-T2 and 3,5-T2AM, respectively.

Interestingly, the other diiodothyronamines, 3,3′-diiodothyronamine (3,3′-T2AM) and 3′,5′-diiodothyronamine (3′,5′-T2AM) do not undergo deiodination by naphthyl-based deiodinase mimics under physiologically relevant conditions (Fig. S30C and D, ESI†). One of the monoiodo derivatives, 3-iodothyronamine (3-T1AM) and the completely deiodinated derivative, thyronamine (T0AM) are detected in the blood plasma of several organisms.[5a] Biosynthesis of 3-T1AM from T4 has recently been shown to occur in the intestinal tissue, and this process involves both the decarboxylation by ornithine decarboxylase (ODC) and deiodination by DIOs.[16] Although 3,5-T2AM undergoes deiodination by the deiodinase mimics to produce 3-T1AM, 3-T1AM has been found to be completely stable in the presence of small molecule deiodinase mimics (Fig. S30E, ESI†). The other monoiodo derivative, 3′-iodothyronamine (3′-T1AM) also does not undergo biomimetic deiodination to produce T0AM (Fig. S30F, ESI†). It should be noted that 3-T1AM undergoes tyrosyl ring deiodination by DIO3 to form T0AM but 3′-T1AM does not undergo phenolic ring deiodination by DIO1.[8]

As Se···I halogen bonding was proposed to be responsible for the deiodination of thyroid hormones and their metabolites,[9c] we carried out detailed density functional theory (DFT) calculations to understand the strength of the halogen bond formed by THs and TAMs, and to understand the origin of differences in the reactivity of THs and TAMs towards deiodination reactions. Theoretical studies and experimental evidence suggest that the electron density is anisotropically distributed around the halogen atom in organic halides and because of this, a region of positive electrostatic potential is present on the tip of the C–X (X = halogen) covalent bond (σ-hole). The σ-hole is surrounded by an electro-neutral ring followed by a belt of negative potential coaxial with the C–X bond.[17] The presence of the σ-hole on the halogen atoms is responsible for the formation of the halogen bond in the presence of electron donors.[18] Natural bond orbital (NBO) calculations on 3,5-T2 indicated the positive charges on the tyrosyl ring iodine atoms at 0.201 and 0.199 arbitrary units (a.u.). To understand the potential of the iodine atoms to form halogen bonding with selenium, 3,5-T2 was optimized with a model selenolate, methyl selenolate ($MeSe^-$), using B3LYP hybrid functional and 6-31+G* basis sets for all the atoms except iodine for which the 6-311G** basis set was used. As expected, the optimised geometry exhibited a strong Se···I halogen bonding between 3,5-T2 and $MeSe^-$. The non-bonded distance between selenium and iodine atoms in the halogen-bonded geometry (3,5-T2·$MeSe^-$), 2.962 Å, has been found to be almost 23.7% shorter than the sum of their van der Waals radii (3.880 Å) (Fig. 5A). Furthermore, the C–I bond in 3,5-T2 (2.127 Å) is elongated by almost 0.199 Å in 3,5-T2·$MeSe^-$ (2.326 Å). Similar DFT calculations on 3,5-T2AM indicated the positive charge on both the tyrosyl ring iodine atoms at 0.199 a.u. Interestingly, the Se···I distance in the halogen-bonded geometry between 3,5-T2AM and $MeSe^-$ (3,5-T2AM·$MeSe^-$) has been found to be 2.975 Å (Fig. 5B), which is higher than that observed in 3,5-T2·$MeSe^-$. In agreement with this, the C–I bond elongation in 3,5-T2AM·$MeSe^-$, 0.191 Å (C–I bond length: 2.127 Å in 3,5-T2AM; 2.318 Å in 3,5-T2AM·$MeSe^-$) is less than that observed in 3,5-T2·$MeSe^-$. NBO calculations on the halogen-bonded geometries afforded the Se···I interaction energies at 57.79 kcal mol^{-1} and

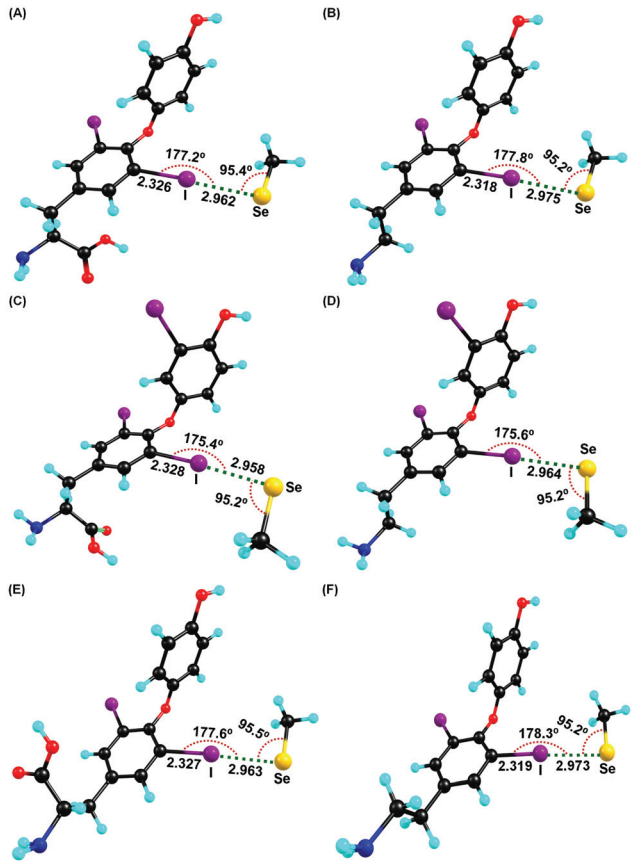

Fig. 5 A comparison of the Se···I distances, C–I bond lengths (Å) and C–I–Se and C–Se–I angles (°) in the halogen bonded adducts formed by the tyrosyl ring iodine atoms of *transoid* conformations of 3,5-T2 (A), 3,5-T2AM (B), T3 (C), T3AM (D), and *cisoid* conformations of 3,5-T2 (E) and 3,5-T2AM (F) with $MeSe^-$.

55.07 kcal mol^{-1} for 3,5-T2 and 3,5-T2AM, respectively, indicating that the decarboxylated metabolite, 3,5-T2AM forms weaker halogen bonding interactions with selenium than 3,5-T2. Similar results were obtained for the halogen-bonded geometries formed by the tyrosyl ring iodine atoms of T3 and T3AM (Fig. 5C and D). The Se···I non-bonded distances were found to be 2.958 Å and 2.964 Å in T3·$MeSe^-$ and T3AM·$MeSe^-$, respectively. NBO calculations on these halogen-bonded geometries afforded the Se···I halogen bonding interaction energies at 58.68 kcal mol^{-1} and 57.33 kcal mol^{-1} for T3·$MeSe^-$ and T3AM·$MeSe^-$, respectively, suggesting that T3 and T3AM form stronger halogen bonding with selenium than 3,5-T2 and 3,5-T2AM, respectively.

Although thyroid hormones are known to exist both in the *cisoid* and *transoid* conformations, *transoid* is the most stable conformation.[19] The amino acid side chain and phenolic ring of THs remain in the same face and opposite faces of the plane of the tyrosyl ring in the *cisoid* and *transoid* conformers, respectively. We have recently shown that the strength of halogen bonding formed by the iodine atoms of thyroid hormones can be altered by changing the conformation.[20] Therefore, we calculated the Se···I interaction energies also in the *cisoid* conformations of THs and TAMs. Interestingly, the interaction energies are slightly different for the *cisoid* and *transoid* conformations. For example, the strength of the halogen bond formed by the *cisoid* geometries of 3,5-T2 and 3,5-T2AM (Fig. 5E and F) is found to be 57.66 kcal mol^{-1} and 55.4 kcal mol^{-1}, respectively. Nevertheless, the calculations both in the *cisoid* and *transoid* geometry of THs and TAMs follow a similar trend in the strength of Se···I halogen bonding, and these interaction energies may be attributed to the faster deiodination of thyroid hormones (T3, 3,5-T2) than iodothyronamines (T3AM, 3,5-T2AM) as well as the faster deiodination of triiodo derivatives (T3, T3AM) than the diiodo derivatives (3,5-T2, 3,5-T2AM) (Fig. 3, 4C and Table S1, ESI†). In addition to the Se···I interaction energies, intermolecular dimerisation of T3 in solution with the help of hydrogen bonding and I···I halogen bonding has been shown to enhance the rate of deiodination of the same by organoselenium compounds.[9d] Similarly, intermolecular interactions in solution may also play an important role in the initial rate of deiodination of 3,5-T2 and 3,5-T2AM by deiodinase mimics.

Enzymatic deiodinations of THs are known to be highly pH-sensitive. pH can alter the regioselectivity as well as the rate of deiodination of THs by DIOs. For example, while DIO1 catalyzes the phenolic ring deiodination of T4 to produce T3 at physiological pH, it catalyzes the tyrosyl ring deiodination of T3 to produce 3,3′-T2 at alkaline pH. In contrast, DIO3 and its Cys mutant do not catalyze the phenolic ring deiodination of T4, T3 and rT3 over a wide pH range although the rate of deiodination by DIO3 has been found to be enhanced at alkaline pH. In our previous report on the biomimetic deiodination of THs, we have also shown that the tyrosyl ring deiodination of T3 by compound **3** is sensitive to pH of the reaction mixture.[9b] However, the effect of pH on the regioselectivity and the rate of deiodination of TAMs by DIOs is not known. In the present study, we have investigated the effect of pH on the deiodination of T3AM and 3,5-T2AM by compound **9**. Deiodination of both T3AM and 3,5-T2AM by compound **9** was found to be extremely slow at acidic pH. However, the initial rate of deiodination of T3AM and 3,5-T2AM by compound **9** to produce 3,3′-T2AM and 3-T1AM,

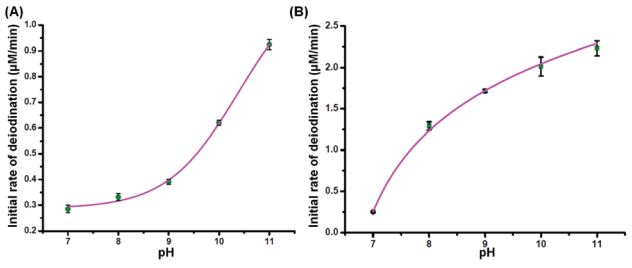

Fig. 6 Variation in the initial rate of deiodination of T3AM (A) and 3,5-T2AM (B) by compound **9** with increasing pH. Assay conditions: T3AM or 3,5-T2AM (0.3 mM), compound **9** (1.2 mM), dithiothreitol (DTT) (15 mM), sodium borohydride ($NaBH_4$) (30 mM), sodium phosphate buffer (100 mM), 20% acetonitrile (v/v), 37 °C.

respectively, was observed to significantly increase over the pH range 7–11 (Fig. 6). Interestingly, in both cases, the regioselectivity of deiodination was not altered at alkaline pH. These observations are very similar to those observed for the deiodination of T4 and T3 by DIO3 and deiodinase mimics. Increase in the rate of deiodination at alkaline pH may be attributed to the increased nucleophilicity of selenolate and thiolate groups, which are produced by sequential deprotonation of selenol groups in **9** and thiol groups in dithiothreitol (DTT), respectively, at higher pH.

Conclusions

In this paper, we have discussed the biomimetic deiodination of THs and their decarboxylated metabolites, TAMs by a series of naphthalene-based organoselenium compounds. The selenium-containing compounds used in the present study have secondary amine, primary alcohol and thioacetal substitutions in the close proximity of one of the selenium atoms. The activity of all of these compounds in deiodinating THs and TAMs is found to be higher than the unsubstituted compound, naphthalene-1,8-diselenol (compound **3**). The deiodinase activity of these compounds has been explained on the basis of Se···X (X = N, O and S) noncovalent interactions although it is also found to be dependent on the nature of iodinated substrates. THs undergo faster deiodination than TAMs by these naphthyl-based small molecules. Furthermore, the deiodination of the triiodo derivatives is found to be faster than that of the diiodo derivatives. Theoretical investigations on the formation of Se···I halogen bonding indicated that THs form stronger halogen bonding with selenium than TAMs. Also the triiodo derivatives form stronger Se···I halogen bonding than the diiodo derivatives. Altogether, the deiodination of THs and TAMs by naphthyl-based selenium-containing small molecules depends on the strength of the Se···I halogen bond and intramolecular Se···X (X = N, O and S) noncovalent interactions.

Experimental section

Deiodination assays

The deiodination reactions of thyroid hormones and iodothyronamines were performed in a mixture of 20% v/v acetonitrile and phosphate buffer (100 mM, pH 7.00) at 37 °C in the presence of 15 mM dithiothreitol (DTT). Due to the low solubility of iodothyronamines in phosphate buffer at physiological pH, 20% acetonitrile was added to the buffer. The selenols (1.2 mM) were freshly generated in the assay mixture by reducing the corresponding diselenides with sodium borohydride ($NaBH_4$). Initial 10–15% conversion of thyroid hormones or iodothyronamines to the deiodinated product was monitored to determine the initial rate of deiodination. The deiodinated products were separated by reverse-phase HPLC using a prepacked cartridge (Princeton C18 column, 5 μm, 150 mm × 5 mm) and gradient elution with acetonitrile/ammonium acetate–acetic acid buffer (15 mM, pH 4). The formation of deiodinated products was monitored at λ = 275 nm and they were quantified from the corresponding peak areas. The final assay mixture contained 0.3 mM thyroid hormones or iodothyronamines, 1.2 mM mimic, 15 mM dithiothreitol (DTT), 30 mM sodium borohydride ($NaBH_4$), phosphate buffer (100 mM, pH 7.0) and 20% v/v acetonitrile.

Synthesis

Compounds **11** and **18** (Scheme S1, ESI†) were synthesized by following the literature procedure.[9a–c]

Synthesis of 19. Compound **19** (Scheme S1, ESI†) was obtained as a side-product during the synthesis of **18** by using the Vilsmeier–Haack formylation of naphthalene-1,8-diselenide, **11**[9b] and was purified by column chromatography using 230–400 mesh silica gel as the stationary phase and toluene as the mobile phase. ^{1}H NMR ($CDCl_3$) δ (ppm): 10.17 (S, 1H), 8.97–8.99 (dd, J = 6.8 Hz, 1H), 7.69 (d, J = 7.6 Hz, 1H), 7.46–7.53 (m, 3H); ^{13}C NMR ($CDCl_3$) δ (ppm): 191.7, 153.5, 142.4, 138.9, 138.3, 135.5, 130.9, 128.5, 123.0, 121.6, 120.5; ^{77}Se NMR ($CDCl_3$) δ (ppm): 455, 437.

Synthesis of 12. 2-Amino-2-methylpropan-1-ol (1.43 g, 16 mmol) was added dropwise to a solution of **18** (100 mg, 0.32 mmol) in 25 mL dry acetonitrile and the resulting mixture was refluxed for 24 h. The solvent was evaporated under reduced pressure and the resulting Schiff base (**20**) was reduced without further purification. The Schiff base was dissolved in 1 : 1 chloroform/methanol (30 mL) and was treated with sodium borohydride (242 mg, 6.4 mmol) in small portions. Then the reaction mixture was heated at 50 °C for 5 h followed by evaporation of solvent under reduced pressure. The reaction mixture was dissolved in ethyl acetate and washed with water twice. The organic layer was collected, dried over anhydrous sodium sulphate and evaporated *in vacuo* to afford a viscous liquid. The crude product was then purified by flash chromatography using chloroform/ethyl acetate as the eluent to give **12** as a red coloured viscous liquid in 60% overall yield. ^{1}H NMR ($CDCl_3$) δ (ppm): 7.33–7.41 (m, 3H), 7.13 (t, J = 7.6 Hz, 1H), 6.89 (d, J = 8 Hz, 1H), 3.80 (s, 2H), 3.48 (s, 2H), 2.67 (s, br, 2H), 1.13 (s, 6H); ^{13}C NMR ($CDCl_3$) δ (ppm): 141.3, 140.3, 139.4, 136.7, 134.9, 127.5, 126.7, 125.0, 123.4, 123.1, 69.6, 55.9, 46.9, 30.2, 23.4; ^{77}Se NMR ($CDCl_3$) δ (ppm): 426, 345. ESI-MS (m/z) calcd for $C_{15}H_{17}NOSe_2$ $[M + H]^+$: 387.9719, found 387.9876.

Synthesis of 13. 2-Amino-2-methylpropane-1,3-diol (1.68 g, 16 mmol) was added dropwise to a solution of **18** (100 mg, 0.32 mmol) in 25 mL dry acetonitrile and the resulting mixture was refluxed for 24 h. After removing the solvent under reduced pressure, the resulting Schiff base (**21**) was reduced without further purification. The Schiff base was dissolved in 1 : 1 chloroform/methanol (30 mL) and was treated with sodium borohydride (242 mg, 6.4 mmol) portionwise. Then the reaction mixture was heated at 50 °C for 5 h after which the solvent was evaporated under reduced pressure. The mixture was dissolved in ethyl acetate and washed with water twice, dried over anhydrous sodium sulphate and evaporated

in vacuo to afford a yellowish-red solid. The crude product was then purified by flash chromatography using chloroform/ethyl acetate as the mobile phase to yield **13** as a yellowish red coloured solid in 55% overall yield. ^{1}H NMR (d_6-DMSO) δ (ppm): 7.53 (d, J = 8 Hz, 1H), 7.41 (d, J = 7.6 Hz, 2H), 7.11–7.18 (m, 2H), 3.95 (s, 2H), 3.49 (s, 4H), 1.02 (s, 3H); ^{13}C NMR (d_6-DMSO) δ (ppm): 141.5, 140.1, 139.4, 136.7, 136.5, 128.0, 127.2, 125.2, 123.8, 123.3, 64.6, 59.7, 46.4, 18.1; ^{77}Se NMR (d_6-DMSO) δ (ppm): 439, 342. ESI-MS (m/z) calcd for $C_{15}H_{17}NO_2Se_2$ $[M + H]^+$: 403.9668, found 403.9364.

Synthesis of 14. Compound **14** was synthesized by following a similar procedure reported earlier.[9e] A solution of compound **18** (200 mg, 0.64 mmol) in a mixture of 1 : 3 chloroform and methanol was treated with sodium borohydride (145 mg, 3.84 mmol) in small portions. The reaction mixture was stirred for 1 h at room temperature after which the solvent was evaporated under reduced pressure. Then the viscous slurry was dissolved in dichloromethane, washed thoroughly with water, dried over anhydrous sodium sulphate and evaporated *in vacuo* to afford a brown solid. The crude product was then purified by flash chromatography using chloroform/ethyl acetate as the mobile phase to afford **14** as a brown solid in 95% yield. ^{1}H NMR ($CDCl_3$) δ (ppm): 7.5 (d, J = 8 Hz, 1H), 7.46 (d, J = 8.4 Hz, 1H), 7.40 (d, J = 7.2 Hz, 1H), 7.25 (d, J = 7.2 Hz, 1H), 7.21 (t, J = 8 Hz, 2H), 4.74 (s, 2H); ^{13}C NMR ($CDCl_3$) δ (ppm): 140.9, 140.6, 138.8, 137.5, 134.0, 127.8, 127.1, 124.9, 123.7, 122.0, 66.2; ^{77}Se NMR ($CDCl_3$) δ (ppm): 411, 406. ESI-MS (m/z) calcd for $C_{11}H_8OSe_2$ $[M + Na]^+$: 338.88, found 338.96.

Synthesis of 15. 3-Mercaptopropanoic acid (85 mg, 0.8 mmol) was added to a solution of **18** (100 mg, 0.32 mmol) in 20 mL dry dichloromethane and the resulting solution was cooled to 0 °C. Borontrifluoride–diethyl etherate (80 μL, 45–50% solution) was added dropwise to the mixture at 0 °C and the solution was allowed to attain room temperature over 12 h. Then the reaction mixture was extracted with ethyl acetate (20 mL, 3×) and the combined organic layers were washed thoroughly with water, dried over anhydrous sodium sulphate and evaporated under reduced pressure to afford a dark brown-colored liquid. The crude product was then purified by reverse-phase flash chromatography using a pre-packed C18 silica cartridge and water/methanol as the mobile phase to yield **15** as a dark red liquid in 45% yield. ^{1}H NMR (d_4-MeOH) δ (ppm): 7.54 (d, J = 8 Hz, 1H), 7.44–7.47 (dd, J = 2.8 Hz, 2H), 7.36 (d, J = 8.4 Hz, 1H), 7.24 (t, J = 7.6 Hz, 1H), 5.43 (s, 1H), 2.84–2.95 (m, 2H), 2.70–2.79 (m, 2H), 2.62–2.67 (m, 4H); ^{13}C NMR (d_4-MeOH) δ (ppm): 174.5, 141.6, 141.3, 139.6, 137.4, 133.5, 128.9, 127.9, 125.0, 123.2, 122.5, 55.6, 34.3, 28.2; ^{77}Se NMR ($CDCl_3$) δ (ppm): 446, 390. ESI-MS (m/z) calcd for $C_{17}H_{16}O_4S_2Se_2$ $[M - H]^-$: 506.8742, found 506.7935.

Synthesis of 16. Compound **16** was synthesized following the procedure reported earlier.[9d] A mixture of **18** (100 mg, 0.32 mmol) and 1,2-ethanedithiol (46 mg, 0.49 mmol) in 20 mL dry dichloromethane was treated with borontrifluoride–diethyl etherate (80 μL, 45–50% solution) dropwise at 0 °C. The reaction mixture was allowed to attain room temperature over 12 h. Then the mixture was diluted with excess dichloromethane, thoroughly washed with water, dried over anhydrous sodium sulphate and concentrated *in vacuo* to yield a dark brown coloured liquid. The crude product was then purified by column chromatography using petroleum ether/diethyl ether as the mobile phase to afford **16** as a dark brown solid in 35% yield. ^{1}H NMR ($CDCl_3$) δ (ppm): 7.51 (d, J = 8.4 Hz, 1H), 7.44 (t, J = 6.8 Hz, 2H), 7.33 (d, J = 8 Hz, 1H), 7.24–7.28 (q, J = 5.6 Hz, 1H), 5.87 (s, 1H), 3.61–3.67 (m, 2H), 3.41–3.45 (m, 2H); ^{13}C NMR ($CDCl_3$) δ (ppm): 141.4, 141.3, 139.7, 137.6, 132.9, 129.1, 128.0, 125.2, 123.6, 122.8, 58.9, 41.0; ^{77}Se NMR ($CDCl_3$) δ (ppm): 453, 382.

Synthesis of 17. A mixture of **18** (100 mg, 0.32 mmol) and 1,2-ethane dithiol (46 mg, 0.49 mmol) in 20 mL dry dichloromethane was treated with borontrifluoride–diethyl etherate (80 μL, 45–50% solution) dropwise at 0 °C. The reaction mixture was stirred for 12 h at room temperature. Then the mixture was diluted with excess dichloromethane, thoroughly washed with water, dried over anhydrous sodium sulphate and concentrated *in vacuo* to yield a dark brown liquid. The crude product was then purified by column chromatography using petroleum ether/diethyl ether as the mobile phase to afford **17** as a dark brown solid in 40% yield. ^{1}H NMR ($CDCl_3$) δ (ppm): 7.49 (d, J = 8 Hz, 1H), 7.43 (t, J = 6.8 Hz, 2H), 7.31 (d, J = 8.4 Hz, 1H), 7.22–7.27 (m, 1H), 5.86 (s, 1H), 3.59–3.65 (m, 2H), 3.39–3.45 (m, 2H); ^{13}C NMR ($CDCl_3$) δ (ppm): 141.5, 141.3, 139.7, 137.6, 132.9, 129.2, 128.0, 125.2, 123.6, 122.8, 58.9, 41.0; ^{77}Se NMR ($CDCl_3$) δ (ppm): 453, 381. ESI-MS (m/z) calcd for $C_{13}H_{10}S_2Se_2$ $[M]^+$: 389.8554, found 389.8551.

Synthesis of iodothyronamines. All the nine iodothyronamines (T4AM, T3AM, rT3AM, 3,3′-T2AM, 3,5-T2AM, 3′,5′-T2AM, 3-T1AM, 3′-T1AM and T0AM) were synthesized following a literature procedure reported by Scanlan *et al.*[21] with minor modifications.

T4AM. *N*-*t*-BOC-3,3′,5,5′-tetraiodothyronamine (200 mg, 0.24 mmol) was treated with a 1 : 4 v/v mixture of trifluoroacetic acid and dichloromethane and the solution was stirred for 1 h at room temperature. The solvent was evaporated *in vacuo* to yield a yellowish white sticky solid, which was purified by reverse-phase HPLC using a C18 column (Atlantis, 250 × 19 mm, 10 μm) and 70% methanol/water as the eluent, to afford T4AM as a white solid in 90% yield. ^{1}H NMR (d_4-MeOH) δ (ppm): 7.89 (s, 2H), 7.10 (s, 2H), 3.22 (t, J = 7.6 Hz, 2H), 2.94 (t, J = 7.6 Hz, 2H); ^{13}C NMR (d_4-MeOH) δ (ppm): 153.3, 151.6, 150.7, 141.0, 138.6, 126.2, 91.1, 84.7, 40.4, 31.8; ESI-MS (m/z) calculated for $C_{14}H_{11}NO_2I_4$ $[M + H]^+$: 733.7047, found 733.9314.

T3AM. T3AM was synthesized using *N*-*t*-BOC-3,3′,5-triiodothyronamine (200 mg, 0.28 mmol) by following a similar procedure described for T4AM. Yield: 92%. ^{1}H NMR (d_4-MeOH) δ (ppm): 7.89 (s, 2H), 7.00 (d, J = 2.8 Hz, 1H), 6.78 (d, J = 8.8 Hz, 1H), 6.64–6.67 (dd, J = 6.4 Hz, 1H), 3.23 (t, J = 8 Hz, 2H), 2.95 (t, J = 7.2 Hz, 2H); ^{13}C NMR (d_4-MeOH) δ (ppm): 153.9, 152.5, 149.9, 141.0, 138.2, 125.6, 116.8, 115.0, 91.4, 83.4, 40.5, 31.8; ESI-MS (m/z) calculated for $C_{14}H_{13}NO_2I_3$ $[M + H]^+$: 607.8080, found 607.7704.

rT3AM. rT3AM was synthesized using *N*-*t*-BOC-3,3′,5′-triiodothyronamine (200 mg, 0.28 mmol) by following a similar procedure described for T4AM. Yield: 95%. ^{1}H NMR (d_4-MeOH) δ (ppm): 7.85 (s, 1H), 7.31 (s, 3H), 6.91 (d, J = 8.4 Hz, 1H), 4.64 (br, s, 2H), 3.19 (t, J = 7.6 Hz, 2H), 2.94 (t, J = 7.6 Hz, 2H); ^{13}C NMR (d_4-MeOH) δ (ppm): 156.0, 152.6, 151.3, 140.5, 135.0, 130.7, 129.0, 119.8, 88.8, 84.5, 40.7, 32.3; ESI-MS (m/z) calculated for $C_{14}H_{13}NO_2I_3$ $[M + H]^+$: 607.8080, found 607.7794.

3,3′-T2AM. 3,3′-T2AM was synthesized using *N*-*t*-BOC-3,3′-diiodothyronamine (200 mg, 0.34 mmol) by following a similar procedure described for T4AM. Yield: 93%. ^{1}H NMR (d_4-MeOH) δ (ppm): 7.81 (d, J = 2 Hz, 1H), 7.22–7.24 (q, J = 4 Hz, 2H), 6.84 (t, J = 2.8 Hz, 1H), 6.78 (d, J = 8.4 Hz, 1H), 3.16 (t, J = 8 Hz, 2H), 2.91 (t, J = 7.6 Hz, 2H); ^{13}C NMR (d_4-MeOH) δ (ppm): 157.0, 153.9, 149.9, 140.3, 133.9, 130.4, 129.4, 120.2, 118.5, 115.1, 88.0, 83.4, 40.8, 32.3; ESI-MS (m/z) calculated for $C_{14}H_{14}NO_2I_2$ $[M + H]^+$: 481.9114, found 481.8453.

3,5-T2AM. 3,5-T2AM was synthesized using *N*-*t*-BOC-3,5-diiodothyronamine (200 mg, 0.34 mmol) by following a similar procedure described for T4AM. Yield: 90%. ^{1}H NMR(d_4-MeOH) δ (ppm): 7.86 (s, 2H), 6.70 (d, J = 8.8 Hz, 2H), 6.56 (d, J = 8.8 Hz, 2H), 4.63 (s, br, 2H), 3.31 (t, J = 1.2 Hz, 2H), 2.93 (d, br, J = 6.8 Hz, 2H); ^{13}C NMR (d_4-MeOH) δ (ppm): 154.3, 152.5, 150.0, 140.9, 137.8, 116.3, 115.9, 91.6, 40.5, 31.8; ESI-MS (m/z) calculated for $C_{14}H_{13}NO_2I_2$ $[M + H]^+$: 481.9114, found 481.8681.

3′,5′-T2AM. 3′,5′-T2AM was synthesized using *N*-*t*-BOC-3′,5′-diiodothyronamine (200 mg, 0.34 mmol) by following a similar procedure described for T4AM. Yield: 94%. ^{1}H NMR (d_4-MeOH) δ (ppm): 7.39 (s, 2H), 7.29 (d, J = 8.4 Hz, 2H), 6.96 (d, J = 8.4 Hz, 2H), 3.19 (t, J = 7.6 Hz, 2H), 2.96 (t, J = 8 Hz, 2H); ^{13}C NMR (d_4-MeOH) δ (ppm): 157.1, 152.6, 151.5, 132.1, 130.5, 130.0, 118.9, 84.4, 41.0, 32.9; ESI-MS (m/z) calculated for $C_{14}H_{13}NO_2I_2$ $[M + H]^+$: 481.9114, found 481.8962.

3-T1AM. 3-T1AM was synthesized using *N*-*t*-BOC-3-iodothyronamine (200 mg, 0.56 mmol) by following a similar procedure described for T4AM. Yield: 95%. ^{1}H NMR (d_4-MeOH) δ (ppm): 7.79 (d, J = 2 Hz, 1H), 7.19 (dd, J = 6.4 Hz, 1H), 6.77–6.83 (m, J = 9.2 Hz, 4H), 6.71 (d, J = 8.4 Hz, 1H), 3.14 (t, J = 8 Hz, 2H), 2.88 (t, J = 7.6 Hz, 2H); ^{13}C NMR (d_4-MeOH) δ (ppm): 157.7, 154.3, 149.3, 140.1, 133.1, 130.1, 120.5, 117.6, 116.3, 87.5, 40.8, 32.3; ESI-MS (m/z) calculated for $C_{14}H_{14}NO2I_1$ $[M + H]^+$: 356.0147, found 356.0094.

3′-T1AM. 3′-T1AM was synthesized using *N*-*t*-BOC-3′-iodothyronamine (200 mg, 0.56 mmol) by following a similar procedure described for T4AM. Yield: 91%. ^{1}H NMR (d_4-MeOH) δ (ppm): 7.30 (d, J = 2.8 Hz, 1H), 7.23 (d, J = 8.8 Hz, 2H), 6.88–6.91 (m, J = 2.8 Hz, 3H), 6.83 (d, J = 8.8 Hz, 1H), 3.15 (t, J = 8.4 Hz, 2H), 2.92 (t, J = 8 Hz, 2H); ^{13}C NMR (d_4-MeOH) δ (ppm): 158.0, 153.8, 150.0, 131.2, 130.2, 130.1, 120.9, 118.2, 115.0, 83.3, 41.0, 32.8; ESI-MS (m/z) calculated for $C_{14}H_{14}NO_2I_1$ $[M + H]^+$: 356.0147, found 356.0525.

T0AM. T0AM was synthesized using *N*-*t*-BOC-thyronamine (200 mg, 0.87 mmol) by following a similar procedure described for T4AM. Yield: 96%. ^{1}H NMR (d_4-MeOH) δ (ppm): 7.21 (d, J = 8.4 Hz, 2H), 6.87 (t, J = 10.4 Hz, 4H), 6.79 (d, J = 8.8 Hz, 2H), 3.15 (t, J = 8 Hz, 2H), 2.91 (t, J = 8 Hz, 2H); ^{13}C NMR (d_4-MeOH) δ (ppm): 158.6, 154.1, 149.4, 130.6, 130.1, 121.1, 117.7, 116.2, 41.1, 32.8; ESI-MS (m/z) calculated for $C_{14}H_{15}NO_2$ $[M + H]^+$: 230.1181, found 230.0648.

Single crystal X-ray crystallography

Compound **13** was recrystallized from a 1 : 1 mixture of chloroform–methanol by a slow evaporation method. Yellowish orange coloured crystals were filtered, washed with petroleum ether and dried under high vacuum. Compound **14** was recrystallized from a 1 : 2 mixture of chloroform–methanol by a slow evaporation method. Reddish-brown coloured crystals were filtered, washed with petroleum ether and dried under high vacuum. The single crystal X-ray diffraction data of **13** and **14** were recorded on a Bruker SMART APEX CCD diffractometer utilizing SMART/SAINT software.[22] All the diffraction data were collected at room temperature using graphite-monochromatized Mo-Kα radiation of wavelength 0.71073 Å. SHELX-97 program, incorporated in WinGX, was used to solve the structures. Empirical absorption corrections were assigned with SADABS.[23,24] All the non-hydrogen atoms were refined by anisotropic displacement coefficients. The hydrogen atoms on the carbon, nitrogen and oxygen atoms were included in geometric positions.

Crystal data for 13

$C_{15}H_{17}NO_2Se_2$, F_w = 401.22, monoclinic $P2_1/n$, a = 12.201(4) Å, b = 6.3287(16) Å, c = 19.477(5) Å, α = 90°, β = 96.736(10)°, γ = 90°, V = 1493.6(7) Å^3, Z = 4, MoK$_\alpha$ radiation (λ = 0.71073 Å), T = 296(2) K, ρ_{calcd} (g cm^{-3}) = 1.784, μ(MoK$_\alpha$) (mm^{-1}) = 4.951, collected reflections = 4519, unique reflections = 2688, GOF (F^2) = 1.070, $R_1{}^a$ = 0.0512, w$R_2{}^b$ = 0.1005.

Crystal data for 14

$C_{11}H_8O_1Se_2$, F_w = 314.09, orthorhombic $P2_12_12_1$, a = 4.6505(5) Å, b = 13.4476(13) Å, c = 16.1385(16) Å, α = 90°, β = 90°, γ = 90°, V = 1009.27(18) Å^3, Z = 4, MoK$_\alpha$ radiation (λ = 0.71073 Å), T = 296(2) K, ρ_{calcd} (g cm^{-3}) = 2.067, μ(MoK$_\alpha$) (mm^{-1}) = 7.286, collected reflections = 2297, unique reflections = 1676, GOF (F^2) = 1.208, $R_1{}^a$ = 0.0783, w$R_2{}^b$ = 0.2135.

Computational methods

Gaussian03 and Gaussian09 suites of quantum chemical programme were used to perform all the DFT calculations.[25] All the hormones and hormone metabolites were optimized using the hybrid Becke 3-Lee-Yang-Parr (B3LYP) exchange correlation functional and 6-31+G* basis sets for all the atoms except iodine for which the 6-311G** basis set was used.[26] To ensure that it was a minimum on the potential energy surface, frequency calculations were performed for each optimized geometry at the same level of theory using the same basis sets. Natural Bond Orbital (NBO) calculations[27] were carried out using 6-311+G** basis sets except iodine for which the 6-311G** basis set was used. All the theoretical calculations

have been done on the S-configuration of the thyroid hormones at the chiral centre.

Acknowledgements

This research work was financially supported by the Science and Engineering Research Board (SERB), India. S. Mondal thanks the Indian Institute of Science, Bangalore for a research fellowship and G. Mugesh thanks SERB for the J. C. Bose National Fellowship (Grant No. SB/S2/JCB-067/2015).

References

1 (*a*) R. Mullur, Y. Y. Liu and G. A. Brent, *Physiol. Rev.*, 2014, **94**, 355; (*b*) F. Gentile, R. DiLauro and G. Salvatore, Biosynthesis and Secretion of Thyroid Hormones, in *Endocrinology*, ed. L. J. DeGroot, WB Saunders Company, Philadelphia, 3rd edn, 1995, pp. 517–542; (*c*) S. Mondal, K. Raja, U. Schweizer and G. Mugesh, *Angew. Chem., Int. Ed.*, 2016, **55**, 7606.

2 (*a*) D. Behne, A. Kyriakopoulos, H. Meinhold and J. Köhrle, *Biochem. Biophys. Res. Commun.*, 1990, **173**, 1143; (*b*) J. L. Leonard and T. J. Visser, in *Biochemistry of Deiodination in Thyroid Hormone Metabolism*, ed. G. Hennemann, Marcel Dekker, New York, 1986, p. 189; (*c*) M. J. Berry, L. Banu and P. R. Larsen, *Nature*, 1991, **349**, 438; (*d*) P. R. Larsen and M. J. Berry, *Annu. Rev. Nutr.*, 1995, **15**, 323; (*e*) J. L. Leonard and J. Köhrle, in *Intracellular Pathways of Iodothyronine Metabolism in The Thyroid*, ed. L. E. Braverman and R. D. Utiger, Lippincott-Raven, Philadelphia, 1996, p. 144; (*f*) D. L. St. Germain and V. A. Galton, *Thyroid*, 1997, **7**, 655.

3 (*a*) A. C. Bianco, D. Salvatore, B. Gereben, M. J. Berry and P. R. Larsen, *Endocr. Rev.*, 2002, **23**, 38; (*b*) J. Köhrle, *Methods Enzymol.*, 2002, **347**, 125; (*c*) G. G. J. M. Kuiper, M. H. A. Kester, R. P. Peeters and T. J. Visser, *Thyroid*, 2005, **15**, 787.

4 (*a*) T. J. Visser and C. H. H. Schoenmakers, *Acta Med. Austriaca*, 1992, **19**, 18; (*b*) J. Köhrle, *Mol. Cell. Endocrinol.*, 1999, **151**, 103; (*c*) J. Köhrle, F. Jakob, B. Contempré and J. E. Dumont, *Endocr. Rev.*, 2005, **26**, 944.

5 (*a*) T. S. Scanlan, K. L. Suchland, M. E. Hart, G. Chiellini, Y. Huang, P. J. Kruzich, S. Frascarelli, D. A. Crossley II, J. R. Bunzow, S. Ronca-Testoni, E. T. Lin, D. Hatton, R. Zucchi and D. K. Grandy, *Nat. Med.*, 2004, **10**, 638; (*b*) K. P. Doyle, K. L. Suchland, T. M. P. Ciesielski, N. S. Lessov, D. K. Grandy, T. S. Scanlan and M. P. Stenzel-poore, *Stroke*, 2007, **38**, 2569.

6 R. Zucchi, G. Chiellini, T. S. Scanlan and D. K. Grandy, *Br. J. Pharmacol.*, 2006, **149**, 967.

7 A. N. Snead, M. S. Santos, R. P. Seal, M. Miyakawa, R. H. Edwards and T. S. Scanlan, *ACS Chem. Biol.*, 2007, **2**, 390.

8 S. Piehl, T. Heberer, G. Balizs, T. S. Scanlan, R. Smits, B. Koksch and J. Köhrle, *Endocrinology*, 2008, **149**, 3037.

9 (*a*) D. Manna and G. Mugesh, *Angew. Chem., Int. Ed.*, 2010, **49**, 9246; (*b*) D. Manna and G. Mugesh, *J. Am. Chem. Soc.*, 2011, **133**, 9980; (*c*) D. Manna and G. Mugesh, *J. Am. Chem. Soc.*, 2012, **134**, 4269; (*d*) S. Mondal and G. Mugesh, *Chem. – Eur. J.*, 2014, **20**, 11120; (*e*) D. Manna, S. Mondal and G. Mugesh, *Chem. – Eur. J.*, 2015, **21**, 2409; (*f*) S. Mondal, D. Manna and G. Mugesh, *Angew. Chem., Int. Ed.*, 2015, **54**, 9298.

10 Crystallographic data of **13** and **14** have been deposited with the Cambridge Crystallographic Data Centre as supplementary publication no. 1486468 and 1486467, respectively.

11 J. D. Baxter and P. Webb, *Nat. Rev. Drug Discovery*, 2009, **8**, 308.

12 A. S. Padron, R. A. L. Neto, T. U. Pantaleão, M. C. de S. dos Santos, R. L. Araujo, B. M. de Andrade, M. da S. Leandro, J. P. S. W. de Castro, A. C. F. Ferreira and D. P. de Carvalho, *J. Endocrinol.*, 2014, **221**, 415.

13 S. G. Ball, J. Sokolov and W. W. Chin, *J. Mol. Endocrinol.*, 1997, **19**, 137.

14 A. Lanni, M. Moreno, A. Lombardi, P. de Lange, E. Silvestri, M. Ragni, P. Farina, G. C. Baccari, P. Fallahi, A. Antonelli and F. Goglia, *FASEB J.*, 2005, **19**, 1552.

15 (*a*) K. Sorimachi and H. J. Cahnmann, *Horm. Metab. Res.*, 1979, **11**, 233; (*b*) K. Sorimachi and J. Robbins, *Biochim. Biophys. Acta*, 1979, **583**, 443.

16 C. S. Hoefig, T. Wuensch, E. Rijntjes, I. Lehmphul, H. Daniel, U. Schweizer, J. Mittag and J. Köhrle, *Endocrinology*, 2015, **156**, 4356.

17 (*a*) P. Politzer and J. S. Murray, An Overview of σ-Hole Bonding, an Important and Widely-Occurring Noncovalent Interaction, in *Practical Aspects of Computational Chemistry Methods, Concepts, and Applications*, ed. J. Leszczynski and M. K. Shukla, Springer, Heidelberg, 2009, ch. 6; (*b*) T. Clark, M. Hennemann, J. S. Murray and P. Politzer, *J. Mol. Model.*, 2007, **13**, 291.

18 P. Metrangolo, F. Meyer, T. Pilati, G. Resnati and G. Terraneo, *Angew. Chem., Int. Ed.*, 2008, **47**, 6114.

19 (*a*) V. Cody, *Acta Crystallogr., Sect. B: Struct. Crystallogr. Cryst. Chem.*, 1981, **37**, 1685; (*b*) N. Camerman and A. Camerman, *Science*, 1972, **175**, 764; (*c*) V. Cody and W. L. Duax, *Science*, 1973, **181**, 757.

20 (*a*) S. Mondal and G. Mugesh, *Angew. Chem., Int. Ed.*, 2015, **54**, 10833; (*b*) U. Schweizer and C. Steegborn, *Angew. Chem., Int. Ed.*, 2015, **54**, 12856.

21 M. E. Hart, K. L. Suchland, M. Miyakawa, J. R. Bunzow, D. K. Grandy and T. S. Scanlan, *J. Med. Chem.*, 2006, **49**, 1101.

22 A. Altomare, G. Cascarano, C. Giacovazzo and A. Gualardi, *J. Appl. Crystallogr.*, 1993, **26**, 343.

23 G. M. Sheldrick, *Acta Crystallogr., Sect. A: Fundam. Crystallogr.*, 1990, **46**, 467.

24 G. M. Sheldrick, *SHELX-97, Program for the Refinement of Crystal Structures*, University of Göttingen, Göttingen, Germany, 1997.

25 (*a*) M. J. Frisch, G. W. Trucks, H. B. Schlegel, G. E. Scuseria, M. A. Robb, J. R. Cheeseman, J. A. Montgomery Jr., T. Vreven, K. N. Kudin, J. C. Burant, J. M. Millam, S. S. Iyengar, J. Tomasi, V. Barone, B. Mennucci, M. Cossi, G. Scalmani, N. Rega, G. A. Petersson, H. Nakatsuji, M. Hada, M. Ehara, K. Toyota, R. Fukuda, J. Hasegawa, M. Ishida, T. Nakajima, Y. Honda, O. Kitao, H. Nakai, M. Klene, X. Li, J. E. Knox, H. P. Hratchian, J. B. Cross, C. Adamo, J. Jaramillo, R. Gomperts, R. E. Stratmann, O. Yazyev, A. J. Austin, R. Cammi, C. Pomelli, J. W. Ochterski, P. Y. Ayala, K. Morokuma, G. A. Voth, P. Salvador, J. J. Dannenberg, V. G. Zakrzewski, S. Dapprich, A. D. Daniels, M. C. Strain, O. Farkas, D. K. Malick, A. D. Rabuck, K. Raghavachari, J. B. Foresman, J. V. Ortiz, Q. Cui, A. G. Baboul, S. Clifford, J. Cioslowski, B. B. Stefanov, G. Liu, A. Liashenko, P. Piskorz, I. Komaromi, R. L. Martin, D. J. Fox, T. Keith, M. A. Al-Laham, C. Y. Peng, A. Nanayakkara, M. Challacombe, P. M. W. Gill, B. Johnson, W. Chen, M. W. Wong, C. Gonzalez and J. A. Pople, *Gaussian 03, Revision C.02*, Gaussian, Inc., Wallingford CT, 2004; (*b*) M. J. Frisch, G. W. Trucks, H. B. Schlegel, G. E. Scuseria, M. A. Robb, J. R. Cheeseman, G. Scalmani, V. Barone, B. Mennucci, G. A. Petersson, H. Nakatsuji, M. Caricato, X. Li, H. P. Hratchian, A. F. Izmaylov, J. Bloino, G. Zheng, J. L. Sonnenberg, M. Hada, M. Ehara, K. Toyota, R. Fukuda, J. Hasegawa, M. Ishida, T. Nakajima, Y. Honda, O. Kitao, H. Nakai, T. Vreven, J. A. Montgomery Jr., J. E. Peralta, F. Ogliaro, M. Bearpark, J. J. Heyd, E. Brothers, K. N. Kudin, V. N. Staroverov, R. Kobayashi, J. Normand, K. Raghavachari, A. Rendell, J. C. Burant, S. S. Iyengar, J. Tomasi, M. Cossi, N. Rega, N. J. Millam, M. Klene, J. E. Knox, J. B. Cross, V. Bakken, C. Adamo, J. Jaramillo, R. Gomperts, R. E. Stratmann, O. Yazyev, A. J. Austin, R. Cammi, C. Pomelli, J. W. Ochterski, R. L. Martin, K. Morokuma, V. G. Zakrzewski, G. A. Voth, P. Salvador, J. J. Dannenberg, S. Dapprich, A. D. Daniels, Ö. Farkas, J. B. Foresman, J. V. Ortiz, J. Cioslowski and D. J. Fox, *Gaussian 09, Revision A.1*, Gaussian, Inc., Wallingford CT, 2009.

26 (*a*) A. D. Becke, *J. Chem. Phys.*, 1993, **98**, 5648; (*b*) C. Lee, W. Yang and R. G. Parr, *Phys. Rev. B: Condens. Matter*, 1988, **37**, 785.

27 (*a*) A. E. Reed, L. A. Curtiss and F. Weinhold, *Chem. Rev.*, 1988, **88**, 899; (*b*) E. D. Glendening, J. E. Reed, J. E. Carpenter and F. Weinhold, *NBO Program 3.1*, Madison, WI, 1988.